DOI: 10.13009/EUCASS2017-106

Numerical simulation of solid-fuel ramjet combustor with a flame holder

S A Rashkovskiy, S E Yakush* and A A Baranov***
**Institute for Problems in Mechanics of the Russian Academy of Sciences*
Ave. Vernadskogo 101 Bldg 1, Moscow, 119526, Russia
***Bauman Moscow State Technical University*
Baumanskaya 2-ya 5, Moscow, 105005, Russia

Abstract

A computational model of solid-fuel ramjet combustor with a flame holder (a profiled fuel channel) is developed. The polymethylmethacrylate (PMMA) is considered as a solid fuel. Efficiency of the flame holder is determined by the residence time of hot gases in the recirculation zone. The analytical and computational models for solid-fuel ramjet combustor are developed and applied to the analysis of combustion stability. Effect of flame holder size on combustion stability is investigated. Numerical results obtained are analyzed from the point of view of finite residence time, similar to the classical theory of perfectly stirred reactor.

1. Introduction

Solid fuel ramjet engines (SFRE) are promising propulsion systems for unmanned aerial vehicles. The fuels used in these engines do not contain (or contain insufficient amount of) oxidizer, relying on the ambient air oxygen for combustion; therefore, in contrast to rocket fuels, they are not capable of self-sustained burning.

In SFRJ, solid fuel is gradually decomposed by the hot gas flow in the combustion channel, producing flammable vapor which reacts in the gas phase providing the engine thrust. The thermal feedback between the reacting gas flow and solid fuel gasification is, thus, the principal physical and chemical mechanism governing the SFRJ performance.

One of the key problems in designing the solid fuel ramjets is to ensure stability of combustion under a wide range of flight conditions. Despite the over forty-year history of SFRJs [1-4], there still remain unresolved problems hindering their more extensive application. This is mainly due to instability of SFRJ operation and also due to a rather narrow range of operating parameters in which stable combustion of solid fuel is possible. The mechanisms of instability onset and development during the forced combustion of solid fuel at high flow speeds are still a subject of experimental and theoretical studies.

In order to stabilize the solid fuel combustion in SFRE, the solid fuel grains with a profiled channel are used. In particular, a ledge is formed in the inlet part of the grain channel that acts as a flame holder. It was established experimentally that steady combustion of solid fuel in SFRE is possible only with certain shapes and sizes of the flame holder, but detailed mechanisms of combustion stabilization still remain rather vague, and no established methods for the choice of appropriate size and shape of the flame holder exists so far.

Numerical methods are increasingly becoming a tool for studying the processes in SFREs [5–8]. In particular, the flame holder effect shape and size effect on the flow structure in a solid fuel ramjet was studied numerically in [6], where the influence of the ratio of the flame holder length to its depth and the angle of slope of the wall at the exit of the flame holder were analyzed. A steady-state gas-dynamic model and steady-state combustion model of solid fuel was used in [6]; it does not allow simulating the occurrence and development of SFRE operation instability. In [7], self-ignition of solid fuel in a ramjet was investigated, but stability of combustion of solid fuels and connection of the stability with the parameters of the flame holder were not considered. In [8], numerical simulation of diffusion combustion zone above the fuel surface is presented.

The purpose of this work is to develop a numerical model and study combustion in solid fuel ramjet under subsonic conditions, with the focus on performance of flame holder at various flow conditions. In what follows, we present the mathematical model, describe in brief its numerical implementation, and present some results demonstrating the features of transient processes in the combustion chamber of a SFRJ with flame holder.

DOI: 10.13009/EUCASS2017-106

2. Computational model

2.1 Problem Formulation

We consider polymethylmethacrylate (PMMA) as a solid fuel, this choice is due to polymers being a popular material for experimental SFRJs [8]. While gasification of PMMA is a chemically complex process producing large number of gaseous species, in this study we take a simple model that PMMA decomposition assuming that its only product is gaseous monomer methylmethacrylate (MMA) with chemical formula $C_5H_8O_2$. Combustion of MMA in the gas phase is described by a single irreversible gross reaction [8, 9]

$$C_5H_8O_2 + 6O_2 \to 5CO_2 + 4H_2O + \Delta H_c \tag{1}$$

The heat of combustion per unit mass of fuel $\Delta H_c = 25.6$ MJ/kg. Kinetics of this reaction is taken from [9], with

$$\dot{\omega}_k = B \cdot T \cdot \frac{s_k}{W_{O_2}} \rho^2 Y_F Y_{O_2} \exp\left(-\frac{E_c}{RT}\right) \tag{2}$$

where $B = 6.6 \cdot 10^6$ [m^3/mol s K] is the pre-exponential factor, $E_c = 144$kJ/mole is the activation energy, s_k is the mass stoichiometric coefficient of *k*-th species, W_{O_2} is the molar mass of oxygen

Multicomponent gas mixture flow is described by the Reynolds-averaged Navier-Stokes equations (RANS) with standard $k-\varepsilon$ turbulence model.

The system of governing equations is as follows

$$\frac{\partial \mathbf{Q}}{\partial t} + \frac{\partial \mathbf{F}_l}{\partial x_l} + \frac{\partial \mathbf{G}_l}{\partial x_l} = \mathbf{S} \tag{3}$$

$$\mathbf{Q} = \begin{pmatrix} \rho \\ \rho u_1 \\ \rho u_2 \\ \rho E \\ \rho Y_1 \\ \dots \\ \rho Y_N \end{pmatrix}, \quad \mathbf{F}_l = \begin{pmatrix} \rho u_l \\ \rho u_1 u_l + p\delta_{1l} \\ \rho u_2 u_l + p\delta_{2l} \\ (\rho E + p) u_l \\ \rho Y_1 u_l \\ \dots \\ \rho Y_N u_l \end{pmatrix}, \quad \mathbf{G}_l = \begin{pmatrix} 0 \\ -\boldsymbol{\tau}_{1l} \\ -\boldsymbol{\tau}_{2l} \\ -u_i \boldsymbol{\tau}_{il} + q_l \\ \rho Y_1 V_{1l} \\ \dots \\ \rho Y_N V_{Nl} \end{pmatrix}, \quad \mathbf{S} = \begin{pmatrix} 0 \\ 0 \\ 0 \\ w\Delta H_c \\ \dot{w}_1 \\ \dots \\ \dot{w}_N \end{pmatrix} \tag{4}$$

where $\mathbf{Q}$ is the vector of conservative variables, $\mathbf{F}$ and $\mathbf{G}$ are the vectors of inviscid and viscous fluxes, $\mathbf{S}$ is the vector of source terms related to chemical reactions. Here, ρ is the density, (u_1, u_2) are the velocity components, p is the pressure, $E = e + \frac{1}{2}\left(u_1^2 + u_2^2\right)$ is the specific total energy, e is the specific internal energy, Y_i are the mass fractions of species $(i = 1, \dots, N)$, $\dot{w}_i$ is the rate of formation (consumption) of *i*-th component of gas mixture (w is the reaction rate with respect to fuel), $\boldsymbol{\tau}$ is the viscous stress tensor, q_l is the heat flux, $V_{k,l}$ is the velocity of diffusion.

The mixture consists of five components, $C_5H_8O_2$, O_2, CO_2, H_2O, N_2, each described by the ideal gas equation of state, the thermal properties (specific heat, internal energy, enthalpy) as functions of temperature are described by polynomials [10]. The temperature of gas mixture was determined from its total energy and composition by solving a corresponding nonlinear equation. Axisymmetric geometry is implied.

Gas-phase turbulent combustion rate is described by the Eddy Dissipation Concept (EDC) model [11] which is implemented in two formulations, assuming infinite-rate and finite-rate chemistry. In the former case, the volumetric turbulent combustion rate is determined by the mixing rate. In the latter case, combustion is assumed to proceed in "fine structures" treated as constant-pressure perfectly stirred reactor (PSR) with finite residence time; the reactor state is calculated with finite-rate chemistry (2) taken into account. The residence time, as well as mass exchange between PSR are dependent on local turbulent characteristics, in this way the EDC model takes into account turbulence-chemistry interaction. An important feature of finite-rate EDC is that under certain conditions (low

DOI: 10.13009/EUCASS2017-106

temperature and small residence time) is predicts extinction of combustion in PSR, translated as an abrupt drop in the turbulent combustion rate. Alternatively, reactor ignition occurs under appropriate conditions. This model feature is very important because it allows us to consider processes of flame blow-off or re-ignition in SFRJ without any additional assumptions on the ignition/extinction conditions.
On the channel boundaries, injection of gaseous fuel occurs due to solid fuel decomposition described by a simple heat balance model: it is assumed that incident heat flux q_s goes into heating of solid material from its initial temperature T_0 to the boiling temperature T_s which is maintained on the surface of decomposing material, as well as to material gasification with respective specific heat ΔH_G:

$$\dot{m} = \frac{q_s}{c_s(T_s - T_0) + \Delta H_G} \tag{5}$$

Here, c_s is the specific heat capacity of solid fuel. The heat flux q_s can generally include the radiation part, but here it is not taken into account due to small sizes of combustor considered. The following properties of PMMA are chosen: density $\rho_s = 1.18$ g/cm^3, boiling temperature $T_s = 200\,^\circ$C, specific heat capacity $c_s = 1500$ J/(kg K), heat of gasification ΔH_G =1591 kJ/kg. Possible incomplete gasification due to charring is not taken into account.
The density of gas produced on the walls was determined for the equation of state for pure fuel, assuming the local gas pressure; the temperature of the injected gas was taken equal to the boiling temperature T_s for PMMA. As a result, the linear local injection velocity was obtained and used as the boundary condition for the normal velocity component on the wall. For the tangential component of gas velocity, standard wall functions were applied which implies the turbulent log-law velocity profile. The heat flux from the gas phase onto the fuel surface, q_s, required in (5) for calculation of gasification rate, was determined from the temperature wall functions.

2.2 Implementation

Flowfield equations are solved in the axisymmetric framework by an explicit finite-volume high-resolution scheme on a uniform Cartesian grid. The "inviscid" fluxes are approximated by a scheme HR-SLAU2 [12] belonging to the AUSM family of numerical schemes. An important feature of HR-SLAU2 scheme is that it falls into the category of "all-speed" numerical schemes owing to special control of numerical dissipation depending on the local Mach number. This is a must for internal flow problems where high-speed (including supersonic) zones can coexist with low-speed (subsonic) zones. Viscous fluxes are approximated by the standard central-difference scheme.
Viscosity, diffusion, and heat conduction terms are approximated by standard second-order central difference scheme. Chemical reactions are taken into account at a separate substep, with Strang splitting to maintain the second-order approximation in time: at each time step chemistry is advanced by half-step, then the gas dynamics solver is called to advance the solution by full time step, after which the chemistry solver is called again to integrate the kinetic equations by another half-step.
The solid fuel surface, generally, does not coincide with cell boundaries of Cartesian grid; also, it can change with time due to fuel burnout. In this work, we apply the "embedded" sharp interface approach [13] in with the internal boundary described by a level-set of a distance function. In the cells located away from the boundary, normal approximations are used, however, in the near-boundary cells operators are modified to take into account that cells are cut by the surface.

2.3 Geometry, initial and boundary conditions

Numerical simulations were carried out for the geometry which resembles closely the one used in the experiments [2, 3]. The combustor is sketched in Fig. 1, with the main parameters listed in Table 1. Simulations were carried out for four lengths on the flame holder L_2 in order to study the effect of geometry on stability of combustion in SFRJ. The short inlet part of the channel (of length L_1) was assumed to be non-reacting (i.e., solid fuel gasification was suppressed there).
The inlet conditions corresponded to air with normal oxygen contents (21% vol.) injected at a given linear velocity v_{in}, temperature T_{in}, and pressure P_{in} through the air inlet. The same pressure was assumed on the outlet boundary, $P_{out} = P_{in}$. Note that, generally, the inlet pressure and temperature, as well as the outlet pressure are determined by flight conditions, as well as by the presence of a nozzle. These factors will be taken into account in future when considering the performance of a whole SFRJ; at the moment, the research focus is on the flame holder behaviour.

DOI: 10.13009/EUCASS2017-106

At the initial instant, the channel was filled with air at the same pressure and temperature as in the inlet. In order to initialize the flowfield, the initial axial velocity was set to 80% of the inlet velocity v_{in} in a cylindrical domain of the diameter equal to that of the inlet; after a while this flow transformed into a regular jet-like flow near the injector, without generating any significant pressure waves in the combustor.

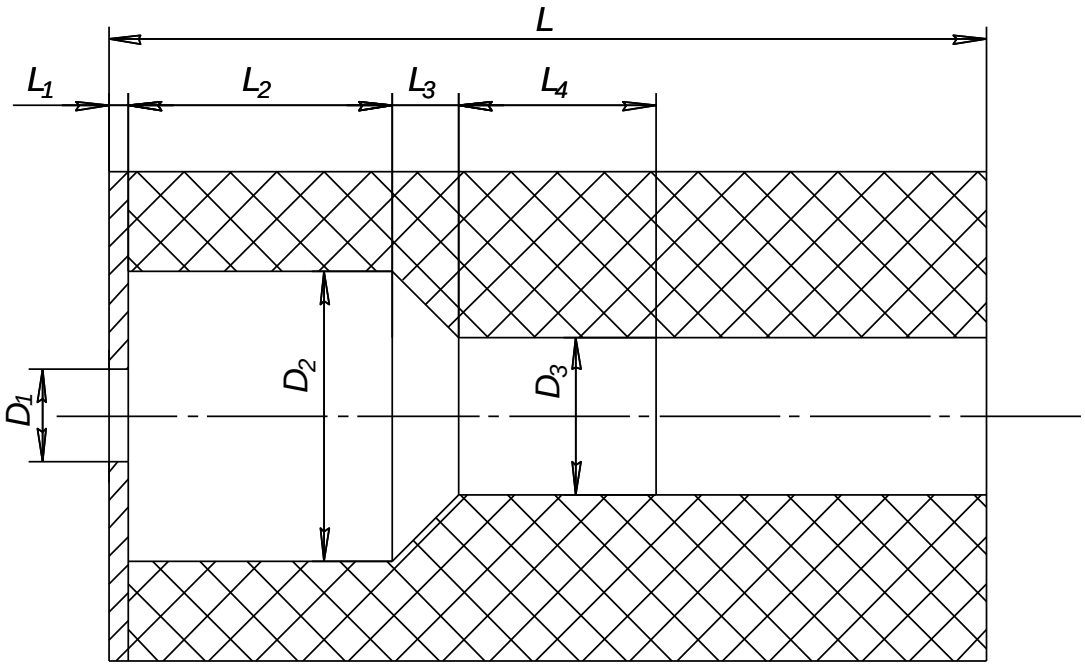

Figure 1: Geometry of solid fuel combustor: air is injected through the inlet of diameter D_1 into the grain channel of diameter D_3 via an expansion chamber of diameter D_2 serving as flame holder due to development of recirculation zone.

Table 1: Dimensions of combustion chamber

Parameter	**Value (mm)**
D_1	10
D_2	30
D_3	15
L	100
L_1	5
L_2	20, 30, 45, 60
L_3	5

"Soft" ignition of fuel was achieved by running the code for the time 5 ms with infinite-rate EDC model. During the initial period of 1 ms, the solid fuel gasification rate (5) was calculated with an artificial constant heat flux $q_s = 1$ kW/m^2, which was sufficient to initialize the gasification, but did not lead to development of high temperature in the combustor. After this period, the heat flux was gradually ramped up over the time of 0.5 ms to its actual local values, and further simulations were carried. Note that in the infinite-rate combustion model the chemical kinetics of gas-phase reaction (1), (2) is not taken into account. Also, the terms limiting the rate due to absence of hot products were switched off for the initial 2 ms, so that fuel was ignited as soon as it mixed with air. This was sufficient to ensure engine ignition for any air flowrate. Note that detailed study of SFRJ start was beyond the scope of the current

DOI: 10.13009/EUCASS2017-106

paper where we focus on possible combustion extinction in an already ignited engine. Specifically, at time of 5 ms, the model was switched from infinite-rate to finite-rate combustion, and subsequent simulation proceeded to time of 20 ms.

Numerical simulations were carried out with the inlet air temperature $T_{in} = 500\,\mathrm{K}$ and pressure $P_{in} = 1$ atm. The inlet velocity v_{in} was set to 100, 200, and 300 m/s, so that only subsonic regimes of SFRJ were considered. In what follows, we consider the results obtained for different length of the flame holder (see Table 1).

2.4 Results

Simulations were carried out with EDC turbulent combustion model with infinite-rate (denoted hereafter by EDC-INF) and finite-rate (EDC-FR) chemistry. Also, it is instructive to compare the results obtained by EDC-INF model with those obtained by well-known Eddy Break-Up (EBU) model which also assumes infinitely-fast chemistry and mixing-controlled combustion rate [14].

Infinite-rate chemistry

As is stated before, for infinite-rate chemistry model the fuel is always ignited at any inlet conditions, and no extinction occurs. In this case, the flow in the engine reaches steady state, therefore, only steady-state distributions are analysed hereafter.

Simulations have shown that both EDC-INF and EDU models give very close results, which is illustrated in Fig.2a-d for the flame holder of length $L_2 = 45\,\mathrm{mm}$ at inlet velocity $v_{in} = 100\,\mathrm{m/s}$. In each subfigure, EBU distributions are shown in the upper half, and EDC-INF in the lower half. Some differences are observed in the temperature (a) and volumetric heat release rate (b) distributions, while differences in the volume fractions of fuel (c) and oxidizer (d) are almost undiscernible. This is further elucidated in Fig. 3a-c, where radial distributions of temperature (a), volumetric heat release rate (b), and species volume fractions are shown in the cross-section running through the middle of flame holder. Evidently, EDC-INF model gives a narrower reaction zone, reflected by a higher flame temperature, otherwise the distributions are very similar. Note that the reaction zone (see Fig. 2b) begins near the inlet where the incoming oxygen reacts with the fuel, due to the assumption of infinite chemical reaction rate.

Finite-rate chemistry

For simulations with finite-rate chemistry, the flowfields obtained with EDC-INF model at time 5 ms were taken as initial conditions, after which the model was switched to EDC-FR. Depending on the inlet velocity and flame holder length, different outcomes were obtained: stable combustion in the whole engine, flame blow-off in the main grain channel with stable combustion in the flame holder, total extinguishment of flame. In what follows, the main findings are summarized.

For the flame holder length of $L_2 = 20\,\mathrm{mm}$ (the shortest one, see Table 1), stable combustion was obtained only for the lowest inlet velocity $v_{in} = 100\,\mathrm{m/s}$; even in this case there was observed a short-time flame extinguishment in the main channel, followed by rapid re-ignition. In the case of higher inlet velocity $v_{in} = 200\,\mathrm{m/s}$, flame extinction occurred in the main channel, while stable combustion was observed in the flame holder. Flame blow-off is shown in Fig. 4a-d by temperature fields at four consequent instants, and in Fig. 5a-d by the volumetric heat release rate distributions at the same instants. Also, streamlines are shown in Fig. 4 which clearly demonstrate the recirculation zone in the flame holder, with no significant vorticity in the main channel. Despite the presence of reaction zone and hot products in the flame holder, no reignition occurs in the main channel due to insufficient heat generated in the flame holder.

A distinct feature of the steady state distributions (Fig. 4d and 5d) is that the reaction zone has detached from the inlet and is “hanging” in the upper part of the vortex. This is due to finite reaction rate taken into account properly in EDC-FR model: the relatively cold air mixes with hot fuel from the recirculation zone, but it takes some induction time for the mixture to start burning in self-sustaining regime. If the inlet velocity is increased, the residence time may become shorter than the induction time, leading to extinguishment of the flame holder itself. This actually was observed in simulations for a higher inlet velocity of 300 m/s where complete flame extinguishment occurred.

The residence time depends not only on the inlet velocity, but also on the distance travelled by the air-fuel mixture, the latter is determined by the length of flame holder. Longer flame holders are more stable in terms of flame blow-off. In particular, it was shown in simulations that for any of the three inlet velocities (from 100 up to 300 m/s), stable combustion was achieved with 45 and 60 mm long flame holders. The steady-state temperature and volumetric heat release rate fields obtained with 45 mm-long flame holder are shown in Figs. 6 and 7 for inlet velocities of 100 and 300 m/s, respectively. One can see that for stable combustion in the channel, a strong enough flow of hot products from the flame holder into the channel is required, not achieved in the case where flame extinguishment occurred (see Figs 4 and 5).

DOI: 10.13009/EUCASS2017-106

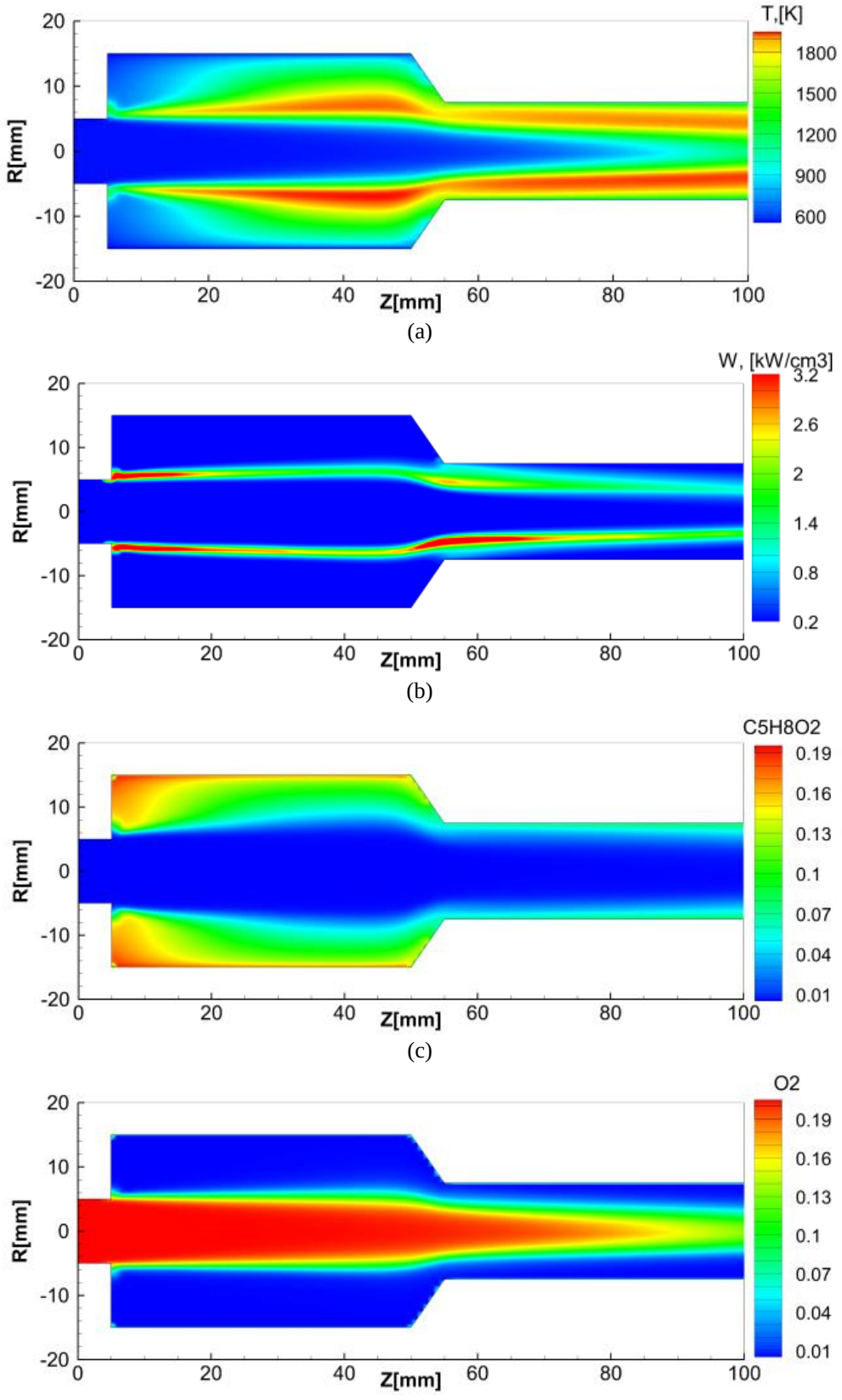

Figure 2: Temperature (a), volumetric heat release rate (b), volume fractions of $C_5H_8O_2$ (c), and O_2 (d) for $P_{in} = 1$ atm, $v_{in} = 100$ m/s, $T_{in} = 500$ K. EBU results are shown in the upper half, EDC-INF are in the lower half of each figure.

DOI: 10.13009/EUCASS2017-106

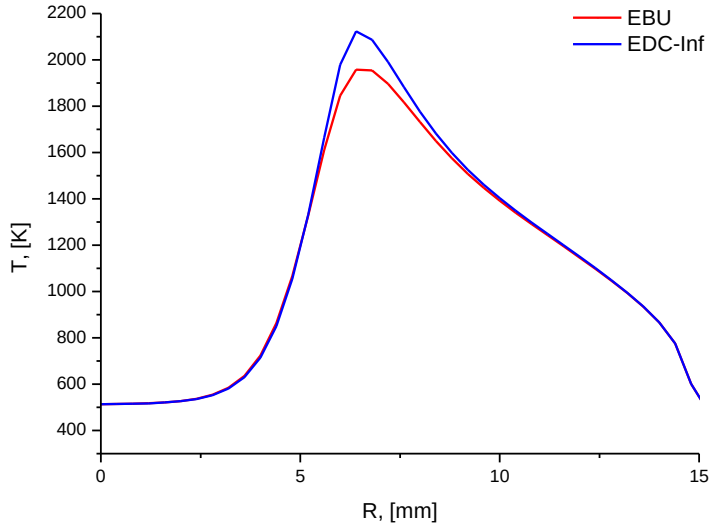

(a)

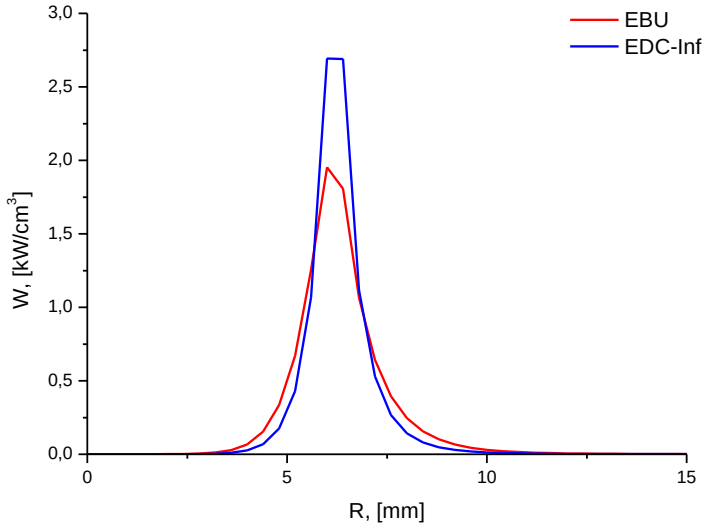

(b)

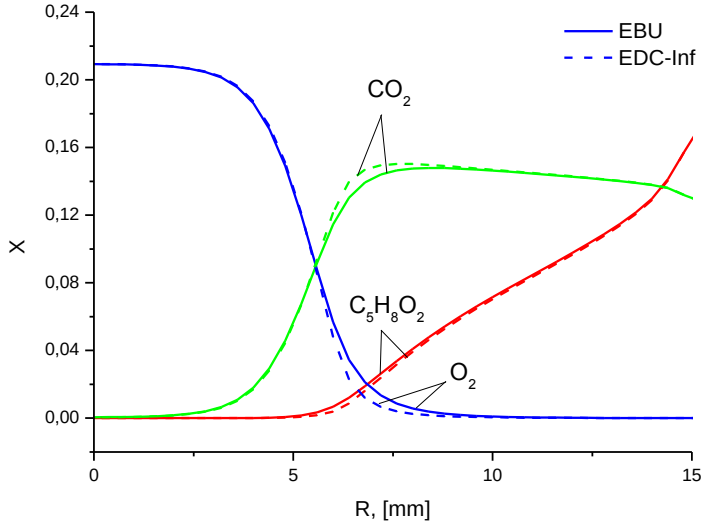

(c)

Figure 3: Temperature (a), volumetric heat release rate (b) and volume fractions of components (c) in the middle of flame holder for $P_{in} = 1$ atm, $v_{in} = 100$ m/s, $T_{in} = 500$ K.

DOI: 10.13009/EUCASS2017-106

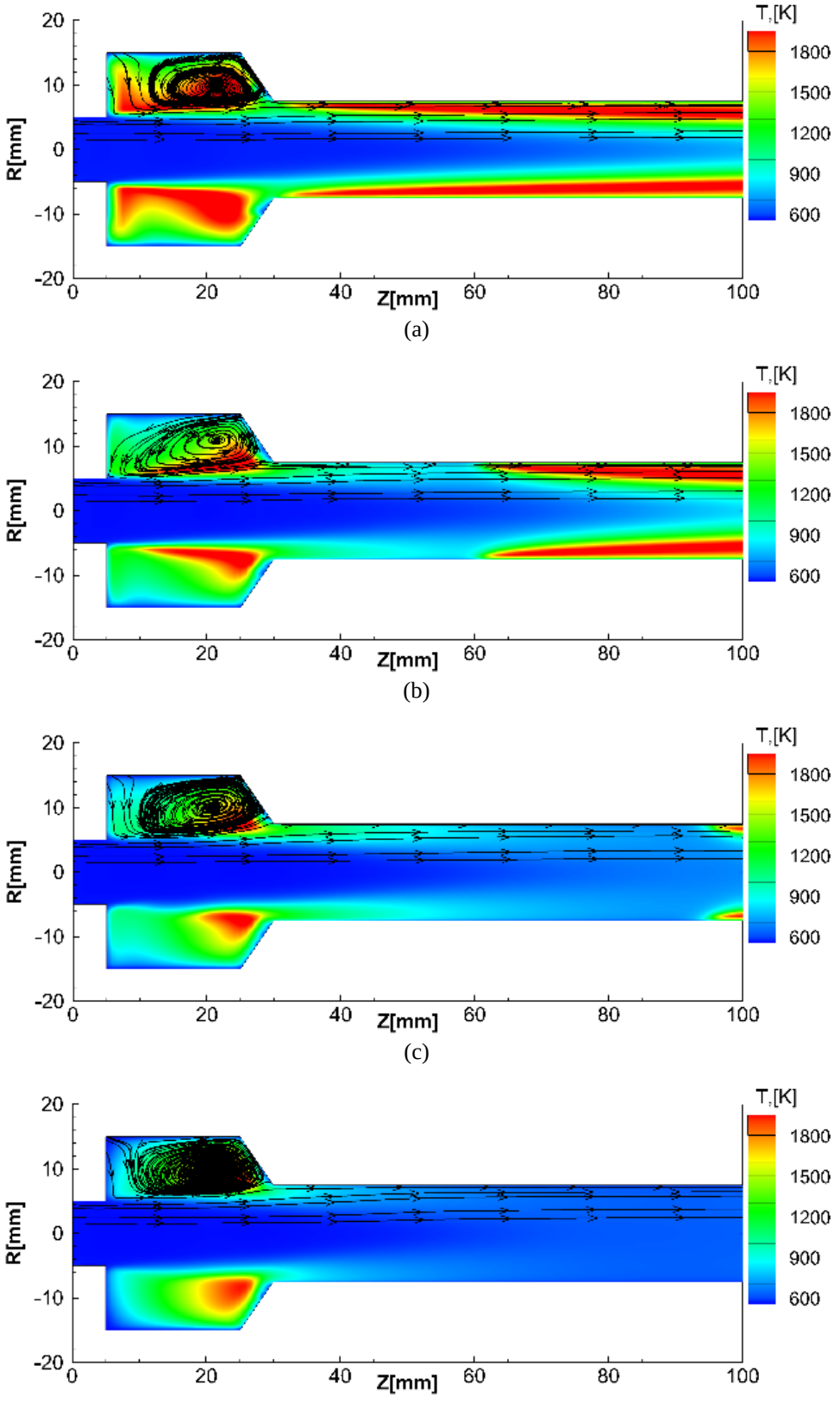

Figure 4: Flame blow-off for 20 mm-long flame holder at $P_{in} = 1$ atm, $v_{in} = 200$ m/s, $T_{in} = 500$ K: temperature shown at times 4 ms (a), 5.5 ms (b), 6 ms (c), 8 ms (d).

DOI: 10.13009/EUCASS2017-106

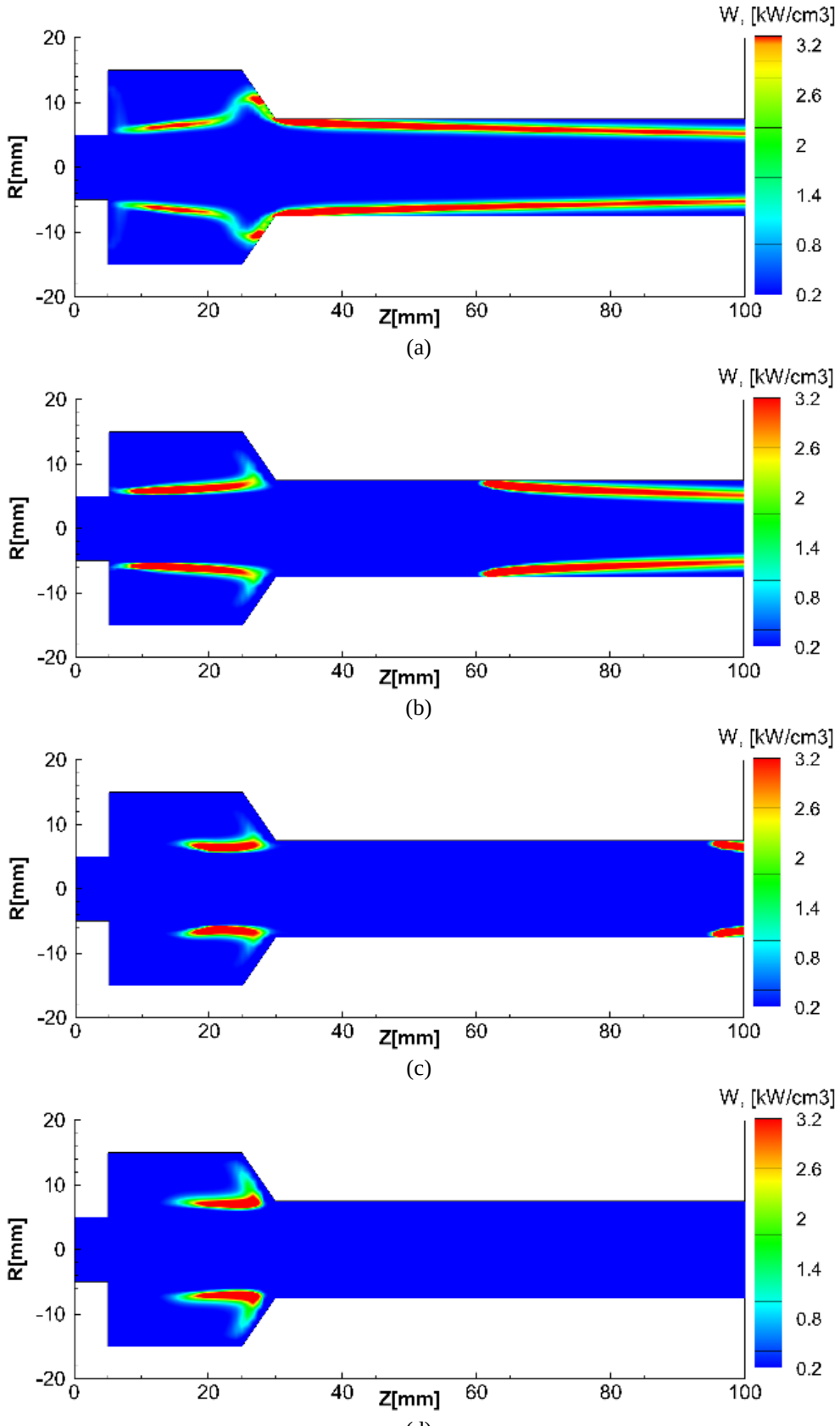

Figure 5: Flame blow-off for 20 mm-long flame holder at $P_{in} = 1$ atm, $v_{in} = 200$ m/s, $T_{in} = 500$ K: volumetric heat release rate shown at times 4 ms (a), 5.5 ms (b), 6 ms (c), 8 ms (d).

DOI: 10.13009/EUCASS2017-106

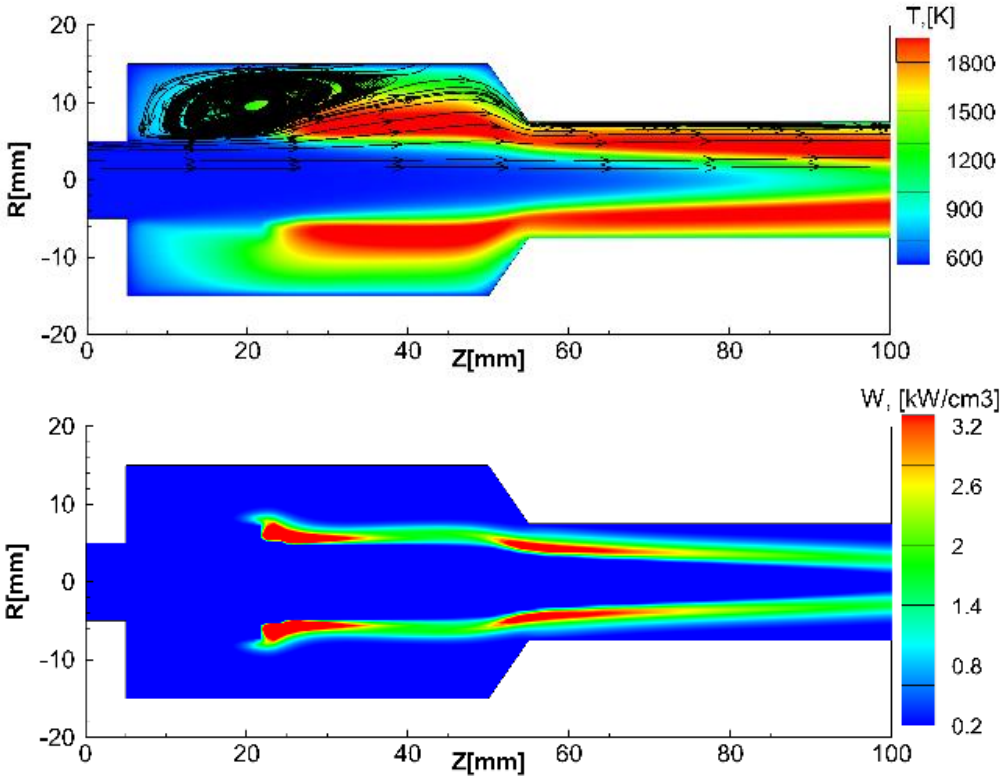

Figure 6: Steady-state temperature (top) and volumetric heat release rate (bottom) fields for 45 mm-long flame holder at $P_{in} = 1$ atm, $v_{in} = 100$ m/s, $T_{in} = 500$ K.

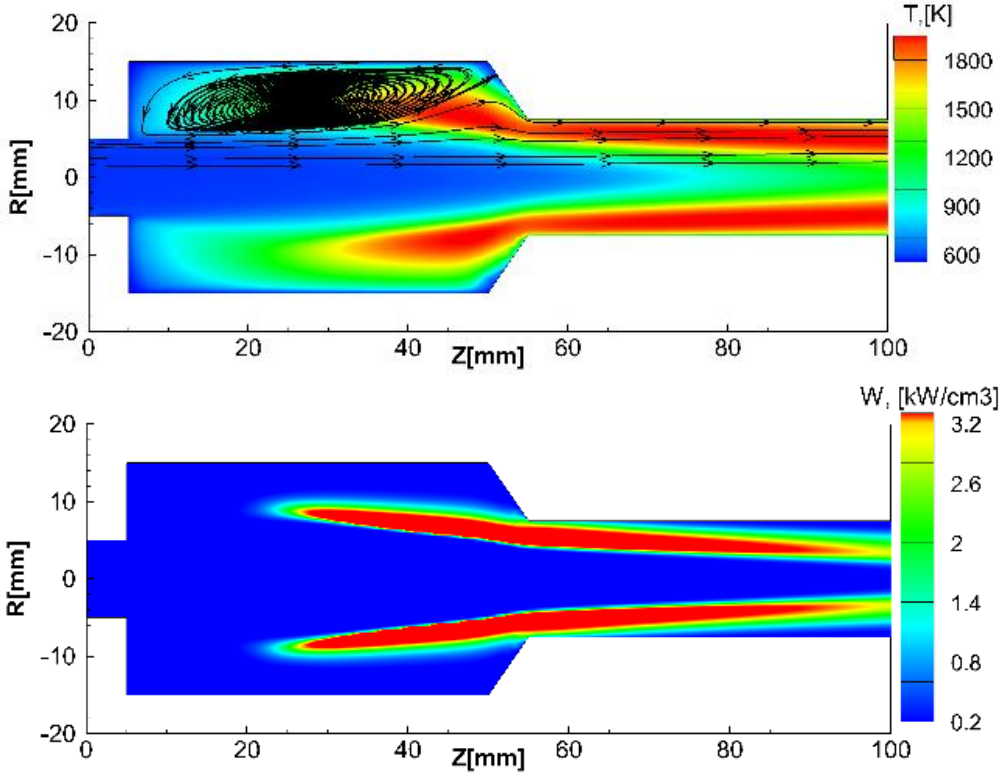

Figure 7: Steady-state temperature (top) and volumetric heat release rate (bottom) fields for 45 mm-long flame holder at $P_{in} = 1$ atm, $v_{in} = 300$ m/s, $T_{in} = 500$ K.

DOI: 10.13009/EUCASS2017-106

4. Conclusions

Thus, it was shown that performance of flame holder in SFRJ is contingent on proper design of its geometry which must on one hand provide conditions for stable combustion in the flame holder itself, and, on the other hand, supply enough hot products into the main channel to avoid flame blow-off. Further research will focus on finding out the stability boundary in a wide range of geometries and operating conditions.

Acknowledgement

This research was supported by Russian Foundation for Basic Research, Grant RFFI 16-29-01084 ofi_m

References

[1] Krishnan, S., and P. George. 1998. Solid fuel ramjet combustor design. *Prog. Aerosp. Sci.* 34:219–256.
[2] Zvuloni, R., A. Gany, and Y. Levy. 1989. Geometric effects on the combustion in solid fuel ramjets. *J. Propulsion.* 5:32–37.
[3] Ben-Yakar, A., B. Natan, and A. Gany. 1998. Investigation of a solid fuel scramjet combustor. *J. Propuls. Power.* 14:447–455.
[4] Gobbo-Ferreira, J., M.G. Silva, and J.A. Carvalho. 1999. Performance of an experimental polyethylene solid fuel ramjet. *Acta Astronaut.* 45:11–18.
[5] Lu, Z., Z. Xia, B. Liu, and Y. Liu. 2015. Experimental and numerical investigation of a solid-fuel rocket scramjet combustor. *J. Propuls. Power*. 31:1–6.
[6] Pei, X., and L. Hou. 2014. Numerical investigation on cavity structure of solid-fuel scramjet combustor. *Acta Astronaut.* 105:463–475.
[7] Chi, H., Z. Wei, L. Wang, B. Li, and Z. Wu. 2015. Numerical investigation of self-ignition characteristics of solid-fuel scramjet combustor. *J. Propuls. Power*. 31:1019–1032.
[8] Novozhilov, V., P. Joseph, K. Ishiko, T. Shimada, H. Wang, and J. Liu. 2011. Polymer combustion as a basis for hybrid propulsion: A comprehensive review and new numerical approaches. *Energies.* 4:1779–1839.
[9] Bedir, H., and J.S. T'ien. 1998. A computational study of flame radiation in PMMA diffusion flames including fuel vapor participation. *Symp. Combust.* 27:2821–2828.
[10] Goos, E., A. Burcat, and B. Ruscic. Extended Third Millennium Ideal Gas and Condensed Phase Thermochemical Database for Combustion with Updates from Active Thermochemical Tables, http://burcat.technion.ac.il/dir/
[11] Gran, I.R., and B.F. Magnussen. 1996. A numerical study of a bluff-body stabilized diffusion flame. Part 2. Influence of combustion modeling and finite-rate chemistry. *Combust. Sci. Technol.* 119:191–217.
[12] Kitamura, K., and A. Hashimoto. 2016. Reduced dissipation AUSM-family fluxes: HR-SLAU2 and HR-AUSM+-up for high resolution unsteady flow simulations. *Comput. Fluids.* 126:41–57.
[13] Hu, X.Y., B.C. Khoo, N.A. Adams, and F.L. Huang. 2006. A conservative interface method for compressible flows. *J. Comput. Phys.* 219:553–578.
[14] Magnussen, B.F., and B.H. Hjertager. 1976. On the mathematical modelling of turbulent combustion with special emphasis on soot formation and combustion. *Sixteenth Symp. (Int.) on Combustion*. 16:719–729.